*Grenze International Journal of Engineering and Technology, Jan Issue*

# Adaptive MPPT Control Approach for Solar PV System

Nalini Karchi[1] and D B Kulkarni[2]
[1]Research Scholar, Dept. of Electrical and Electronics Engineering, KLS GIT
&
[1]Faculty, KLE Dr. MSS College of Engineering and Technology, Belagavi, Karnataka, India
Email: nnnalini2000@rediff.com
[2]Dept of Electrical and Electronics Engineering, KLS Gogte Institute of Technology, Belagavi, Karnataka, India
Email: dbkulkarni@git.edu

***Abstract*—Three different maximum power point tracking controllers are implemented for a solar photovoltaic system. The MPPTs are based on conventional perturb and observe particle swarm optimization and adaptive LMS algorithm. The adaptive MPPT algorithm is developed based on LMS adaptive algorithm. The studied controllers with the system are implemented on MATLAB. The performance is measured in terms of the settling time, peak overshoot, and oscillation. It is observed the system operation is smooth and steady with adaptive controllers.**

***Index Terms*— Controller, Adaptive algorithm, control system, power converter, MPPT, Artificial intelligence algorithm.**

## I. INTRODUCTION

The rising requirement for electrical energy is impacting the environment and power quality. The small generating units based on renewable energy are the best solution to meet the demand for electric power generation. Among all distributed generations, the solar Photovoltaic (PV) system is more famous and reliable. Solar energy is ample and easily available on the earth. This solar energy can be used to generate electricity. The photovoltaic cells are used to convert photo energy into electric energy. A solar photovoltaic array with a power electronic-based converter forms a solar energy conversion system. This system can be operated in standalone or grid-connected form. The PV array is formed by a series and parallel connection of PV modules to generate electricity from a few watts to megawatts. The PV array power at maximum rating can be extracted by using the maximum power point tracking (MPPT) algorithm. There are many MPPT algorithms. They are grouped as conventional form, soft computing approach, and adaptive method. Conventionally developed MPPT algorithms are perturbed and observed (PO), incremental conductance, hill climbing, etc. Soft computing approaches (optimization technique) are differential evolution (DE), particle swarm optimization (PSO), ant colony optimization (ACO), artificial neural network (ANN), cuckoo search, grey wolf, fireflies, etc. These techniques are more suitable for partial shading and change in instance dynamic irradiance. Still, it is hard to manage the computing burden and complexity. Amongst these, the P&O MPPT is simple and easy to implement but exhibits oscillations at the final maximum power point [1]. In this proposed work three different MPPT controllers are developed based on perturbing and observed particle swarm optimization, and an adaptive LMS algorithm. They are implemented with a solar PV system, ‘Fig.2’, and analyzed by implementing them in a MATLAB SIMULINK environment. The paper is arranged in an order such as system development, controller design, simulation and results, and the conclusion.

*Grenze ID: 01.GIJET.9.1.518*

II. FORMULATION OF SYSTEM

## *A. Modeling and Selection of PV system*

The electrical equivalent model of the PV cell is shown in the figure. The solar cell parameters are modeled as a diode in parallel with a constant current source, shunt resistor, and series resistor [2].

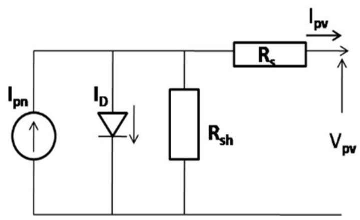


Figure 1: Electric equivalent model of PV Cell

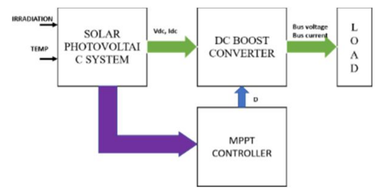


Figure 2. Block Diagram of Standalone Solar PV system with DC Converter

The current $I_{pv}$ is generated by a solar panel. It is a function of series resistors $R_s$, parallel resistors $R_p$, $V_{pv}$, $I_{pn}$, and $I_o$, as follows

$$I_{pv} = I_{ph} + I_o\left[e^{\frac{V_{pv}+R_s I_{pv}}{V_t\, a}} - 1\right] - \frac{V_{pv}+R_s I_{pv}}{R_p} \quad (1)$$

Here,

$I_{pv}$ is the photovoltaic current due to irradiation. If the solar panel is composed of $N_p$ cells in parallel, then $I_{ph} = I_{ph}$,cell x $N_p$. Here $I_{ph}$,cell= saturation current of for a single cell (light generated current $I_L$).

$I_o$= Saturation current of the panel,

$I_o$= $I_o$,cell* $N_p$, Io, the cell is current of a single, cell, and $N_p$ is the number of cells in parallel form

$$V_t = \frac{N_s x K x T}{q} \quad (2)$$

Where, $V_t$=thermal potential of the panel

$N_s$= number of cells in series, K= Boltzmann constant [1.3806503x10-23J/K], q= charge of an electron [1.60217646x10-19C], T= temperature of the p-n junction in Kelvin degree [°K], assumed ambient temperature, a= ideal constant of the diode, Vpv= voltage across the panel, Ns, Number of series-connected modules per string, $V_{dc}$ is the output voltage of PV array, and $V_{mp}$ is the voltage at maximum power. Np, the Number of strings in parallel is obtained as (4) [2] [3].

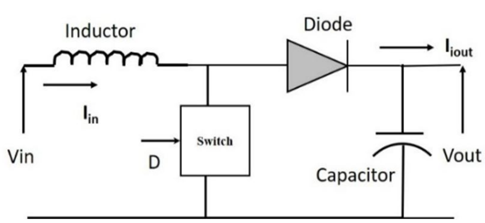


Figure 3. Electrical Circuit diagram of DC Boost Converter

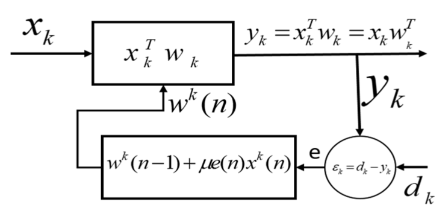


Figure. 4. An Adaptive Finite Impulse Filter Structure.

## *B. Design and selection of DC Boost Converter*

The boost converter is used to extract maximum power from the PV array to feed to the utility or grid. The DC boost converter steps up the input voltage into a higher-level voltage value. The Boost converter is shown in 'Fig.3'. The parameter of this converter is found in (6), and (7).

$$N_s = \frac{V_{dc}}{V_{mp}} \quad (3)$$

$$N_P = \frac{P_{max}/V_{dc}}{I_{mp}} \quad (4)$$

$$D = 1 - \frac{V_{in}}{V_o} \quad (5)$$

$$L_{dcbus} = \frac{V_{in}(V_o - V_{in})}{F_{sw}(\Delta I * V_o)} \quad (6)$$

$$C_{dcbus} = \frac{I_{in}(V_o - V_{in})}{F_{sw}(\Delta V * V_o)} \quad (7)$$

$V_{in}$ is the input voltage to the converter, $V_o$ is the output voltage of the boost converter, P is the rated power of the converter, $F_{sw}$ is the switching Frequency, $\Delta I$ is the current ripple, $\Delta V$ is Voltage ripple, $I_{in}$ is the input current, $I_o$ is the output current, D is the duty cycle.

## III. CONTROL SCHEME

In a Solar PV generation plant, the peak power is extracted through the MPPT based on P-O and Incremental conductance, etc. The output of the MPPT algorithm is the duty cycle value, which is an input to the switch used in the boost converter. The MPPT algorithms are tried based on ‘perturb and observe’ (PO), particle swarm optimization (PSO), and adaptive Least Mean square (LMS) theory.

### *A. Perturb and Observe MPPT algorithm*

This algorithm includes a perturbation in voltage and a change in power is observed. As per this method, the increase in voltage causes an increment in power if it is on the left side of MPP, and a decrement in power if it is on the right side of the maximum power point on P-V characteristics. It can be implemented through two approaches depending on the selection of control parameters like reference voltage and duty cycle. The algorithm determines the maximum power point by searching dP/dV=0. If power and voltage are not changing the derivative will be zero [2]. The implementation of this algorithm is shown in the flow chart figure. 4.

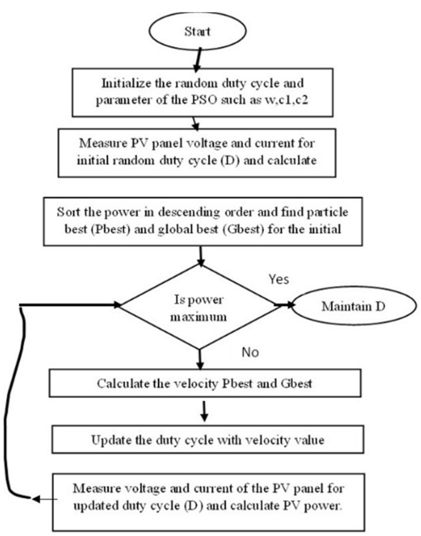


Figure 5. flow diagram of particle swarm optimization algorithm

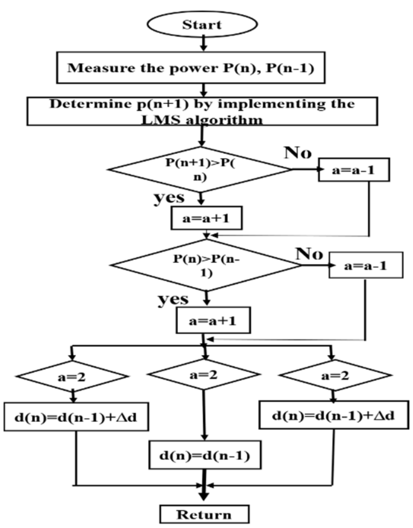


Figure 6. Flow chart of an adaptive LMS- MPPT controller

### *B. Particle Swarm Optimization technique*

This new optimization theory is based on the random search concept. Firstly, it is proposed by Kennedy and Ebahar in 1995. The development of theory includes the behavior of birds. It is applied to determine global optimal results in a discontinuous, nonlinear, non-differential curve. In this algorithm, several particles are used in an ‘n-dimensional’ space. Each particle owns its place, $P_i$, and velocity $V_i$. $P_i$ is distributed randomly and vi, the velocity at its place is zero. The position of the particle is influenced by its best position, $P_{best}$, and the best position of all particles, $G_{best}$. The velocity and position of particles are calculated by

$$V_i^{(k+1)} = \omega V_i^k + C_1 r_2 \left(P_{besti} - P_i^k\right) + C_2 r_2 \left(G_{besti} - P_i^k\right) \quad (8)$$

$$P_i^k = P_i^k + G_i^k \quad (9)$$

The operation of the algorithm is explained in a flow diagram as shown in figure.5 [5,6].

### *C. Adaptive LMS algorithm.*

This adaptive algorithm is neatly explained in the book titled ‘adaptive signal processing’ by author Widrow. The error signal is the performance function. The error is found by comparing the desired signal and the actual signal (feedback). This error function is squared which is also known as mean square error. Later, the gradient of the mean squared error signal is determined with the respective weight function and equated to zero. This will help to find optimal weight function [8].

$$e(n) = d(n) - y(n) \quad (10)$$

$$y(n) = w(n)^T x(n) \quad (11)$$

The input signal is x(n), y(n) is known as an output signal, and w(n) is the weight function. The error signal is e(n).

$$|e(n)^2| = |(d(n) - y(n))|^2 \quad (12)$$

$$w^k(n+1) = w^k(n) + \mu e(n) x^k(n) \quad (13)$$

$$e(n) = p(n) - p(n-1) \quad (14)$$

The operation of the algorithm is to find the weight vector by gradient method towards minimizing the error function. $\mu$= step size in (15). The detailed structure of adaptive FIR is shown in Figure 4. An adaptive LMS - MPPT algorithm is derived by finding the error between the current PV power and previous PV power (14). The power value is predicted by (15). The implementation of the adaptive MPPT control algorithm is carried out as shown in figure 6.

TABLE I. SOLAR PV SYSTEM SPECIFICATIONS

| Sr. No | Description | Specifications |
|---|---|---|
| 1 | Model - Solarland USA SLP215 | |
| 2 | Maximum Power(W) of module | 214.56 |
| 3 | Open circuit Voltage (V), Voc | 36.4 |
| 4 | The voltage at maximum power point (V) | 29.8 |
| 5 | Shunt resistance, (ohm) Rsh | 68.8 |
| 6 | No of strings, $N_p$ | 2 |
| 7 | Cells per module | 60 |
| 8 | Short circuit current (A), $I_{sc}$ | 8 |
| 9 | Current at maximum power point (A), $I_{mp}$ | 7.2 |
| 10 | Series resistance, (ohm), $R_{se}$ | 0.2 |
| 11 | No of the series module, $N_s$ | 2 |
| 12 | The maximum output voltage, $V_{PV}$ (V) | 59.6 |
| 13 | The maximum output power of the panel (W) | 858 |

TABLE II. DC BOOST CONVERTER SPECIFICATION

| Component | Specifications |
|---|---|
| Boost converter Inductor (Henry) | 1.2478e-3 |
| Boost converter capacitor (farad) | 2927e-6 |
| Boost Input capacitor (farad) | 10e-3 |
| Resistive load (R), (ohm) | 76,100 |

$$P(n+1) = P(n-1) + 2\,\mu\, e(n)\, P(n) \quad (15)$$

In this algorithm, the error function is found by measuring the actual PV power and previous power (14). The predicted power value is updated in (15). The predicted power value is compared to the current value of power [9-11]. The operation of an adaptive controller has happened as shown in figure 6.

## IV. SIMULATION AND RESULTS

The implementation of three controllers with a solar PV system and DC boost converter in MATLAB. The system-designed specifications are explained in Table 1 and Table 2. The controllers are tested for different load conditions, solar radiation, and temperature. The results are recorded for PV power, PV voltage, PV current, Load voltage, and load current. The detailed analysis is done for settling time, peak overshoot, and steady-state error.

### *A. Solar insolation is 1000W/m$^2$, the temperature is 25$^0$C, and resistive load is 76 ohms*

The simulation results obtained for this condition are shown in Figure 10 – Figure 12. The data is recorded in Tables 3,4 and 5. Perturb and observe MPPT controller introduces the oscillations of 1507.2 rad/sec at the final value of PV power, where the PV power response due to the PSO controller experiences the peak overshoot of 2.5%. It reaches the first peak value of 880 W at 0.16 sec. The power response due to the PSO MPPT controller reaches its final in lesser time compared to PO-MPPT and Adaptive LMS MPPT controller. The power response obtained by adaptive LMS MPPT is slow but smooth. There are no oscillations in the power response. The

TABLE III. SOLAR PANEL OUTPUT CURRENT (A)

| Time (sec) | LMS0.001 | PSOMPPT | POMPPT | LMS 0.01 |
|---|---|---|---|---|
| 0 | 0 | 0 | 0 | 162.443 |
| 0.1633 | 200 | 273 | 88.8 | 183.93 |
| 0.0303 | 262 | 308 | 162.191 | 225.526 |
| 0.04 | 308 | 480 | 227.995 | 191 |
| 0.05 | 355 | 599 | 312 | 284 |
| 0.06 | 374 | 736 | 362 | 261.382 |
| 0.0963 | 484 | 865 | 447.56 | 386.689 |
| 0.11 | 521 | 878 | 656.49 | 437.302 |
| 0.13 | 587 | 881 | 723.602 | 439.66 |
| 0.16 | 647 | 880 | 821.611 | 551.99 |
| 0.18 | 698.11 | 879 | 874.177 | 592 |
| 0.2 | 723 | 881 | 765 | 628.641 |
| 0.224 | 766 | 876 | 632.549 | 668.36 |
| 0.24 | 803.8 | 879 | 536.067 | 702.295 |
| 0.27 | 839 | 877 | 505.6 | 742.332 |
| 0.29 | 857.49 | 877 | 477 | 775.456 |
| 0.31 | 875.997 | 877 | 477 | 824.165 |
| 0.33 | 880 | 877 | 477 | 858.471 |

TABLE IV. SOLAR PANEL OUTPUT VOLTAGE (V)

| Simulation Time (sec) | LMS MPPT Controller $\mu$=0.001 (Volt) | PSO-MPPT Controller) (Volt) | P&O-MPPT Controller (Volt) | LMS MPPT Controller $\mu$ = 0.01 (Volt) |
|---|---|---|---|---|
| 0 | 0 | 17 | 0 | 10 |
| 0.1633 | 12.52 | 19.2 | 4.63 | 10.38 |
| 0.0303 | 16 | 30 | 12.37 | 14.6489 |
| 0.04 | 19.39 | 35 | 14.4227 | 11.98 |
| 0.05 | 22 | 47.9 | 20.36 | 17.6956 |
| 0.06 | 25 | 58 | 22.6027 | 16.9242 |
| 0.0963 | 30 | 59 | 29.85 | 24.5607 |
| 0.11 | 33 | 89.53 | 41.07 | 27.79 |
| 0.13 | 37.73 | 60.3 | 47 | 31.571 |
| 0.16 | 41 | 61.42 | 53.483 | 35 |
| 0.18 | 44 | 61.79 | 61.733 | 37.88 |
| 0.2 | 46.4 | 62.02 | 65.82 | 40 |
| 0.224 | 49 | 62.22 | 67.9151 | 42.82 |
| 0.24 | 51 | 60 | 69.102 | 45.1867 |
| 0.27 | 54.48 | 59 | 69.39 | 47.88 |
| 0.29 | 56.2 | 58 | 69 | 49.8799 |
| 0.31 | 58.17 | 57 | 67 | 53.4021 |
| 0.33 | 64.15 | 57 | 66 | 56.1865 |
| 0.34 | 68.5 | 56 | 64 | 57.09 |
| 0.5 | 68 | 56 | 61 | 62.2303 |
| 0.6 | 67 | 56 | 56 | 62.14 |

$\mu$= step size in (15)

TABLE V. SOLAR PANEL OUTPUT CURRENT (A)

| Simulation Time (sec) | LMS-MPPT controller $\mu$=0.001 (A) | PSO-MPPT controller (A) | PO-MPPT controller (A) | LMS MPPT controller $\mu$= 0.01 (A) |
|---|---|---|---|---|
| 0 | 0 | 0 | 0 | 0 |
| 0.1633 | 16 | 15.975 | 16 | 16.02 |
| 0.0303 | 15.16 | 15.929 | 16.02 | 15.96 |
| 0.04 | 15.92 | 15.81 | 15.99 | 16.0142 |
| 0.05 | 15.9 | 15.81 | 15.9243 | 15.9496 |
| 0.06 | 15.86 | 15.58 | 15.88 | 15.949 |
| 0.0963 | 15.79 | 15.11 | 15.8047 | 15.8655 |
| 0.11 | 15.71 | 14.4363 | 15.6614 | 15.8291 |
| 0.13 | 15.71 | 14.5659 | 15.58 | 15.78 |
| 0.16 | 15.6 | 14.5659 | 15.4281 | 15.74 |
| 0.18 | 15.62 | 14.774 | 14.0499 | 15.7 |
| 0.2 | 15.59 | 14.3911 | 11.93 | 15.6819 |
| 0.224 | 15.56 | 14.18 | 9.32 | 15.6479 |
| 0.24 | 15.49 | 14.4392 | 7.7 | 15.6163 |
| 0.27 | 14.451 | 14.61 | 7.2 | 15.574 |
| 0.29 | 15.31 | 14.61 | 6.9 | 15.5404 |
| 0.31 | 15.2 | 14.61 | 6.9 | 15.437 |
| 0.33 | 14.12 | 14.61 | 6.9 | 15.2707 |
| 0.34 | 11.4126 | 14.61 | 6.9 | 15.1852 |

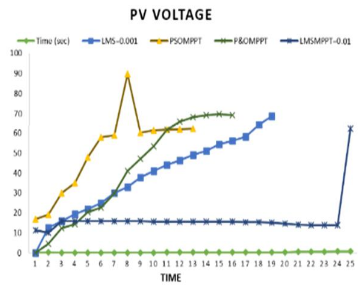


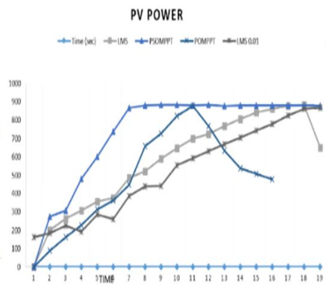


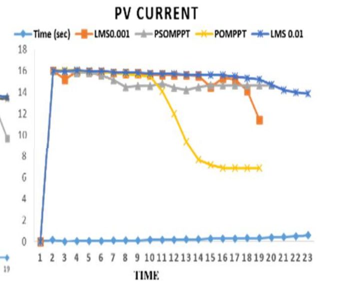


Figure 7. Observed Solar PV Voltage by three controllers

Figure 8. Observed Solar PV Power by three controllers.

Figure 9. Observed Solar PV Current by three controllers.

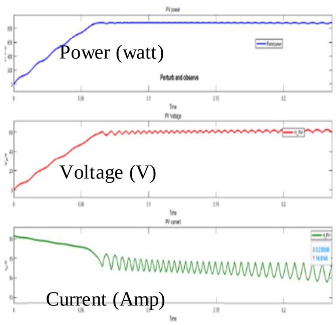


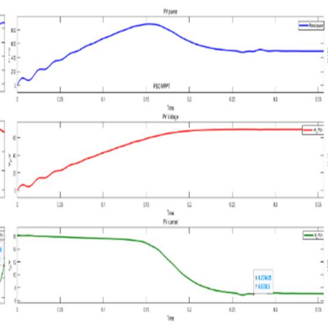

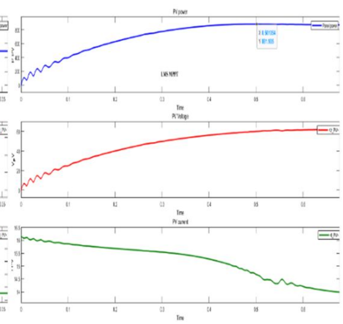

Figure 10. PV Power, PV voltage, PV current observed by Perturb and Observe MPPT (IR=1000W/m$^2$, T=25$^0$C, $R_{load}$=76)

Figure 11. (a) PV Power, (b) PV voltage, (c) PV current observed by PSO MPPT (IR=1000W/m$^2$, T=25$^0$C, $R_{load}$=76)

Figure 12. (a) PV Power, (b) PV voltage, (c) PV current observed by Adaptive LMS MPPT (IR=1000W/m$^2$, T=25$^0$C, $R_{load}$=76)

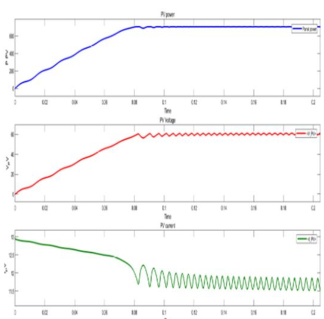

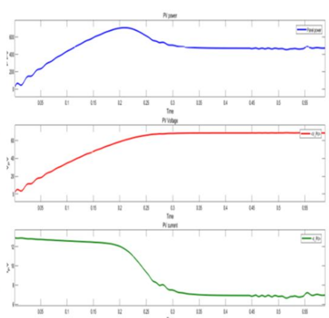

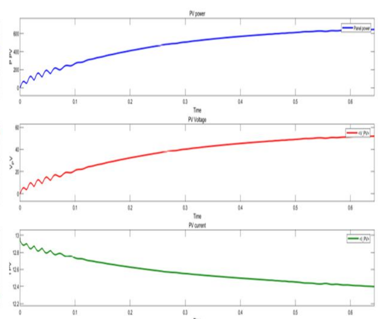

Figure 13. (a) PV Power, (b) PV voltage, and (c) PV current observed by PO MPPT (IR=1000W/m$^2$, T=30$^0$C, $R_{load}$=100).

Figure 14. (a) PV Power, (b) PV voltage, and (c) PV current observed by PSO MPPT (IR=1000W/m$^2$, T=30$^0$C, $R_{load}$=100).

Figure 15. (a) PV Power, (b) PV voltage, and (c) PV current observed by Adaptive LMS MPPT (IR=1000W/m$^2$, T=30$^0$C, $R_{load}$=100).

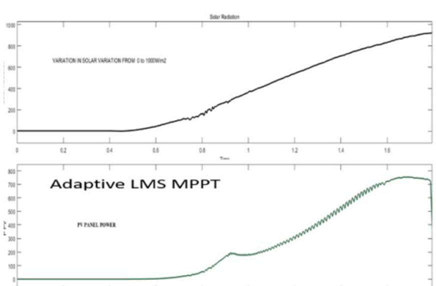


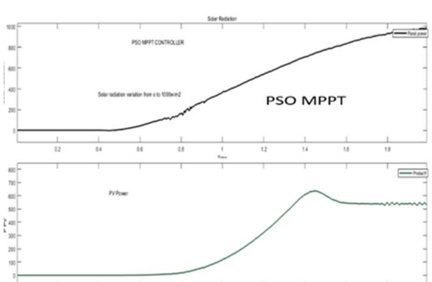


Figure 16. Performance of Adaptive LMS MPPT with variation in solar radiation from 0 to 1000W/m$^2$

Figure 17. Performance of PSO MPPT controller with variation in solar radiation from 0 to 1000W/m$^2$

TABLE VI. SOLAR PANEL POWER, VOLTAGE, CURRENT, DC LINK VOLTAGE AND CURRENT

| Solar radiation=1000 W/m2, T=25, R=76 | | | |
|---|---|---|---|
| Parameter | PSO MPPT Controller | Adaptive LMS MPPT Controller | P&O MPPT Controller |
| $V_{PV}$ (v) | 69.55 | 62.48 | 62.53 |
| $I_{PV}$ (A) | 7.035 | 13.84 | 13.81 |
| $P_{PV}$ (W) | 489 | **864.7** | **863.9** |
| $I_{LOAD}$ (A) | 12.48 | 3.288 | 3.292 |
| $V_{LOAD}$(V) | 188.5 | 249 | 250 |

TABLE VII. SOLAR PANEL POWER, VOLTAGE, CURRENT, DC LINK VOLTAGE AND CURRENT

| Solar radiation=1000 W/m$_2$, T=300C, R=100 ohms | | | |
|---|---|---|---|
| Parameters | PSO MPPT Controller | Adaptive LMS MPPT Controller | P&O MPPT Controller |
| D | 0.6314 | 0.75 | 0.75 |
| $V_{PV}$ (v) | 71.56 | 64.84 | 69.04 |
| $I_{PV}$ (A) | 12.12 | 11.29 | 8.705 |
| $P_{PV}$ (W) | 867 | 735.01 | 670.1 |
| $I_{LOAD}$ (A) | 3 | 2.586 | 1.869 |
| $V_{LOAD}$(V) | 286.7 | 258 | 186.9 |

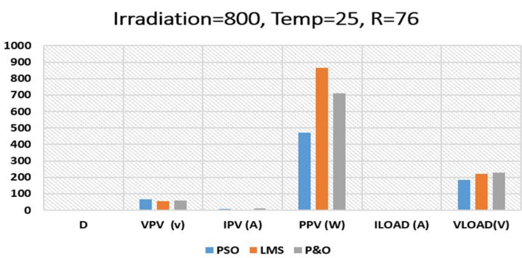


Figure 17. Load voltage, load current observed by PSO MPPT (IR=800W/m$^2$, T=25$^0$C, $R_{load}$=76).

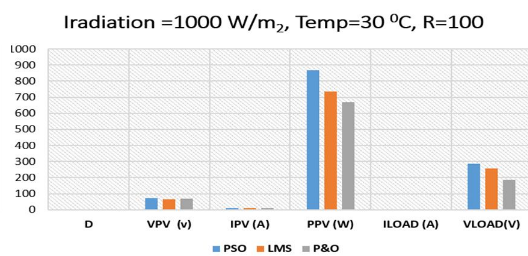


Figure 18. Load voltage, load current observed by PSO MPPT (IR=1000W/m$^2$, T=30$^0$C, $R_{load}$=100 ohm).

TABLE VIII. TRANSIENT AND STEADY-STATE ANALYSIS OF POWER RESPONSE

| Terms | Perturb & observe the controller | PSO controller | Adaptive LMS controller |
|---|---|---|---|
| Settling time (sec) | 0.18 | 0.09630 | 0.33 |
| Rise time (sec) | moderate | fast | slow |
| Peak overshoot (W) | 874.177 | 881 | 857 |
| Steady-state error in % | 5 | 30 | 6 |
| Final Value (W) | 863.9 | 489 | 864.7 |

steady-state error is negligible due to P-O and Adaptive LMS MPPT compared to PSO- MPPT controller. Measured PV power and voltage values are mentioned in Table 3 and Table 4. The current, voltage and power responses observed by the P&O MPPT controller are shown in figure 10 and figure 13 at two different conditions of load. It is observed that initially the response is smooth but later it oscillates at the maximum power point.

In the beginning, fluctuations are found in PV power, PV voltage, and PV current responses, due to the adaptive LMS controller but later smooth response is observed in figure 12. In Figure 11, the speed of response is fast for the PSO MPPT controller compared to the other two controllers. More oscillations are observed in the current response by the PO- MPPT controller once it reaches the final value. It keeps oscillating at the final value. The overall performance out of the three controllers, adaptive LMS controllers prove good controllers. As it reduces the settling time of response, it gives a smooth and steady operation. There are no oscillations, no peak overshoot, and less steady-state error in power response due to adaptive LMS MPPT controller. The step size of this adaptive LMS controller is noticeable. This value affects the performance of the adaptive LMS controller. Results are found for two-step size values 0.01 and 0.001. The adaptive LMS controller performance with step size 0.01 is far better compared to step size 0. 001. The step size is an important factor that needs to be considered seriously while implementing an adaptive LMS controller. The DC link voltage and current are stable and very close to their final value due to PO and adaptive LMS MPPT controller in table 5 and Table 6 and shown in figure 17 and 18.

### *B. Solar insolation is 1000W/m$^2$, the temperature is 30$^0$C, and resistive load is 100 ohms*

For these conditions, the results are shown in figure 13 to figure 15. The oscillations are observed in the PV power, PV voltage, and PV current of the solar PV system. Due to changes in load and solar radiation the oscillations are found in the response due to PO and PSO MPPT controller. Adaptive LMS MPPT controller gives more stable support to the system. The system behavior is unaffected because of the adaptive LMS MPPT controller during a change in solar insolation from 1000 to 800 W/m$^2$, temperature variations, and load conditions. The conventional perturb and observation involves perturbation in the voltage and observing the change in power. In figure 11 and figure 14, one can observe that this (P&O) technique operation is smooth on the left side of the P-V curve, but fluctuations are observed after the maximum power point means the right side of the P-V Curve. Similarly, the response with the PSO MPPT technique includes more up and downs after the maximum PowerPoint. The Adaptive LMS controller provides stability to the system under variations in solar radiation and different conditions as shown in Figure.16.

## V. CONCLUSION

The three MPPT controllers like P&O, PSO and Adaptive MPPT controllers have been developed and implemented with a solar PV panel. The MPPT controllers suggested in the proposed work have proved that maximum power can be extracted by implementing with boost converter integrated solar PV plant. Each one has its advantage and disadvantages. According to the application and situation, they can be implemented. The perturb and observe MPPT is simple and easy to implement. Where PSO MPPT has proved the fastest controller. Sometimes PSO MPPT suffers from convergence and initial parameters. The adaptive LMS MPPT controller is overall good compared to the other two controllers, but the selection of step size (incremental parameter) is a difficult task. The operation of an adaptive LMS MPPT controller for extraction of maximum power point of solar PV panel under variation in solar irradiation was satisfactory with smooth response of power. The advantage of adaptive LMS algorithm is that it calculates the error from desired value and actual value of the system and updates the weights of the function accordingly to reduce the error. The Initialization of parameter burden is reduced. The design and selection of system parameters also influence the operation and performance of the MPPT controllers.

## REFERENCES


[1] S. Mahdi, A.K. Mohamad, S. Saon, T.Tuwoso, Hakkun Elmunsyah, S.W. Mudjanarko, 'Maximum power point tracking using perturb and observe, fuzzy logic and ANFIS' AN Applied Sciences, 2020, doi.org/10.1007/s42452-019-1886-1.

[2] Sihem Elhelali, Noureddine Hidouri, Lassaad Sbita,' A controlled topology for a grid-connected photovoltaic system', International Conference on Control, Engineering and Technology, Vol.3, pp-33-38,2013.

[3] Carlos Andres Ramos Paja, Efrain Perez, Daniel Gonzalez Montoya, Carlos E. Carrejo, Adan Simon-Proceedings, 'Modelling of Full Photovoltaic Systems Applied to Advanced Control Strategies', RE&POJ, Vol.1, No.8, April 2010, doi.org/10.24084/repgj08.712.

[4] M.A. Elgendy, B. zhawi, and D.J. Atkinson, 'Evaluation of Perturb and Observe MPPT Algorithm Implementation Techniques', 2012, DOI: 10.1049/cp.2012.0156.

[5] Harsh Patel, Rital Gajjar, Rajen Pandya, 'Artificial Intelligence Based MPPT techniques for Solar V System: A Review, Journal of Emerging Technologies and Innovative Research, 2019, ISSN-2349-5162

[6] Magadi S, Mahmoud, Nezar M. Alyyazidi, Mohamed I. Abouheaf,' Adaptive intelligent techniques for microgrid control systems: A survey' Electrical Power and Energy Systems,2017,292-305, doi.org/10.10.16/j-ijepes.2017.02.008.

[7] M.S Hamad, Fahmy, A.M, Mostala Ahmed Abdel-Geliei, M, power Quality Improvement of a Single-phase Grid-Connected PV System with Fuzzy MPPT controller, November 2013, doi:10.1109/IECON.6699411.

[8] Pallavi Verma, Priya Mahajan, Rachana Garg.: 'Smooth LMS-based adaptive control of SV system tied to the grid for enhanced power quality. IET Power Electronics, September 2020.

[9] Tatsuya Hoshikawa, Toru Takeda, and Hiroki Matsumoto,' Motor control algorithm with advantages of PID method and LMS method', Proceedings of International Conference on Technology and Social Science 218 (ICTSS 2018).

[10] Obaidullah Lodin, Inderpreet Kaur, Harpreet Kaur, 'Predictive- P& O MPPT Algorithm for Fast and Reliable Tracking of Maximum Power Point in Solar Energy Systems', Techniques' Journal of Recent Technology and Engineering (IJRTE), ISSN:2277-3878, Volume-7, Issue-6S4, April 2019.
[11] S.K, Kollimalla and M.K. Mishra, 'Variable Perturbation size adaptive P&O MPPT algorithm for sudden changes in irradiance', IEEE Trans Sustain Energy, Vol.5, no.3, pp.718-728, Jul. 2014.